



ISSN: 0067-2904

## Synthesis and Characterization of Nano-Composites of Polypropylene / Cr<sub>2</sub>O<sub>3</sub> Nanoparticles Using Licorice Extract

Mohammed Abdulwahid Abdul-Zahra\*, Nada M. Abbass

Department of Chemistry, College of Science, University of Baghdad, Al-Jadriya campus, Baghdad 10071, Iraq

Received: 14/1/2023 Accepted: 13/3/2023 Published: 29/2/2024

### Abstract

In this work, biosynthesized nanoparticles (Cr<sub>2</sub>O<sub>3</sub>) NPs were extracted by licorice root and proven by AFM technique to have a particle diameter of 14.99 nm. These particles were superimposed on polypropylene, and nanocomposites were synthesized and diagnosed using different techniques, such as FT-IR, SEM, EDS, XRD, TG, DTA, and DSC. To identify the shapes, sizes, and nature of the particles of nanocomposites synthesized in an environmentally friendly way using the mentioned techniques, inhibitory actions of microorganisms were studied using several types of bacteria and fungi. To identify the protective role of environmentally friendly nanoparticles, the antimicrobial activity of the synthesized nanoparticles was characterized by green methods. Antioxidant activity was calculated by DPPH, and acceptable results were obtained for scavenging free radicals.

**Keywords:** Polypropylene, Polymer composite, Green methods, Licorice root, Thermogravimetric analysis.

## تخليق وتوصيف المتراكبات النانوية من البولي بروبيلين واوكسيد الكروم النانوي المحضر بواسطة مستخلص عرق السوس

محمد عبدالواحد عبدالزهرة\* و ندى مطير عباس

قسم الكيمياء، كلية العلوم، جامعة بغداد، الجادرية، بغداد، العراق

### الخلاصة

في هذه العمل، تم استخراج الجسيمات النانوية الحيوية (Cr<sub>2</sub>O<sub>3</sub>) بواسطة جذر عرق السوس، وتم إثباتها بتقنية AFM بقطر جزيئات يبلغ 14.99 نانومتر. تم تركيب هذه الجسيمات على مادة البولي بروبيلين وتم تحضير المتراكبات النانوية وتشخيصها باستخدام تقنيات FT-IR و SEM و EDS و XRD و TG و DTA و DSC، لتحديد أشكال وأحجام و طبيعة جزيئات المركبات النانوية المركبة بطريقة صديقة للبيئة باستخدام التقنيات المذكورة، تمت دراسة الفعاليات المثبطة للحياة الدقيقة باستخدام عدة أنواع من البكتيريا والفطريات. لتحديد الدور الوقائي للجسيمات النانوية الصديقة للبيئة، توصيف النشاط المضاد للميكروبات بواسطة الجسيمات النانوية المركبة بالطرق الخضراء. تم حساب النشاط المضاد للأكسدة بواسطة DPPH، وتم الحصول على نتائج مقبولة لكسح الجذور الحرة.

\*Email: [Nada.m@sc.uobaghdad.edu.iq](mailto:Nada.m@sc.uobaghdad.edu.iq)

## 1. Introduction

Environmentally friendly synthesis (green synthesis) is based on biological systems and plants because it is safe, low cost, harmless, non-toxic to the environment, and less polluting, and we can expand synthesis. Therefore, green synthesis is preferred over a number of other chemical techniques. The salty substances are mediated by the valence states of mono- and di-metals, which change to a zero valence state. The metal atoms bind and the growth phase occurs to form a variety of shapes, and then nanoparticles create and form a morphology mediated by activity. Microorganisms such as algae, fungi, seaweed, and rainfall can be used to synthesize plant receptors and nanoparticles [1,2]. The environmental aspects have attracted the use of plants in the synthesis of nanoparticles in recent years [3]. Glycyrrhiza glabra was selected to be used in the biosynthesis of  $\text{Cr}_2\text{O}_3$  NPs because Glycyrrhiza glabra is one of the natural herbs that are widely used in medicine. This herb belongs to the legume family [4]. Recent studies indicate that nanoparticles and materials containing nanoparticles or nanostructures that are amorphous or crystalline have a size of 100 nanometers, high strength, high surface area, and low weight. One of the most notable characteristics of nanoparticles is that they have a broad absorption spectrum and, depending on their characteristics and shape, a large surface area. Nanoparticles range in size from 100 to 2500 nm, and nanomaterials are the link between atoms and microstructures, indicating that they are close to atomic dimensions. Also, they are reasonably priced and retain all of their light activity even after repeated use [5]. There are numerous additives used in polypropylene materials. Most of the additives are related to the final application of desired properties, such as water resistance (hydrophobicity), increased electrical resistance, or treatment of polypropylene, or both [6,7]. In general, the additives reduce the polypropylene content, and thus the cost of the final materials decreases if the material used and the additives are cheaper than polypropylene [8]. Each material is often added for a specific purpose, such as improving the mechanical qualities, crystallization, or thermal behavior. Besides increasing the thermal and mechanical stability, the additives also affect some other properties, such as the ability to get wet (sometimes stimulating the water-repellent properties of polypropylene films), roughness, permeability, fire resistance, optical properties, electrical and static conductivity, density (foams), and even chemical and biological resistance [9].

## 2. Experimental part

### 2.1. Materials

The chemicals, polypropylene (purity 100%), were purchased from SABIC company. Chrom(III)nitrate nonahydrate  $\text{Cr}(\text{NO}_3)_3 \cdot 9\text{H}_2\text{O}$ , and licorice root were purchased from local markets in Baghdad, Iraq.

### 2.2. Methods

#### 2.2.1. Extraction of (*Glycyrrhiza glabra*) licorice root

After grinding the dried roots, the licorice was extracted by adding the ground powder of the roots (2 g) to distilled water (50 mL) before heating until the boiling point. The extracted solution was then cooled to room temperature and filtered several times using gauze. The filtrate is the aqueous extract of licorice [10].

#### 2.2.2. Biosynthesis of metal oxide-NPs

Chrom(III)nitrate.nonahydrate (700 mg) was gently heated in a small amount of distilled water. The extracted licorice was then added to each sample using a dropper, with gentle heating and stirring. When the color of the solution had changed, the addition was stopped, and the mixture was placed in an oven at 80 °C for drying [10].

### 2.2.3. Preparation of nanocomposite

In a round-bottomed flask, a solution of isotactic polypropylene (5 g) in xylene (20 mL) was heated at 90 °C. After complete dissolution, metal oxide nanoparticles of different weights (g) and contents of nanooxides:polypropylene (1:5) were added to the solution and stirred for 1 hour to ensure mixing. Until a homogeneous mixture of polymer and nano-oxides is obtained, the reaction mixture is transferred to a petri dish and dried in an oven at 80 °C to remove the residue solvent completely from the prepared polymeric matrix [11].

## 3. Results and discussion

### 3.1. AFM of nano-oxide metal particles

The atomic force microscope (AFM) was used to determine topography and to distinguish the surface morphology of Cr<sub>2</sub>O<sub>3</sub> as shown in Figure 1. The grooves are heterogeneous, as can be seen from the 3D image, mainly due to the agglomeration of the oxide nanoparticles. Table 1 shows the size distribution of small particles with different diameters [12, 13].

**Table 1 :** Dimensions of Cr<sub>2</sub>O<sub>3</sub> nanoparticles synthesis

Figure	Nano oxide	Average value (nm)	Minimum (nm)	Maximum (nm)
2	Cr <sub>2</sub> O <sub>3</sub>	14.99	14.22	25.57

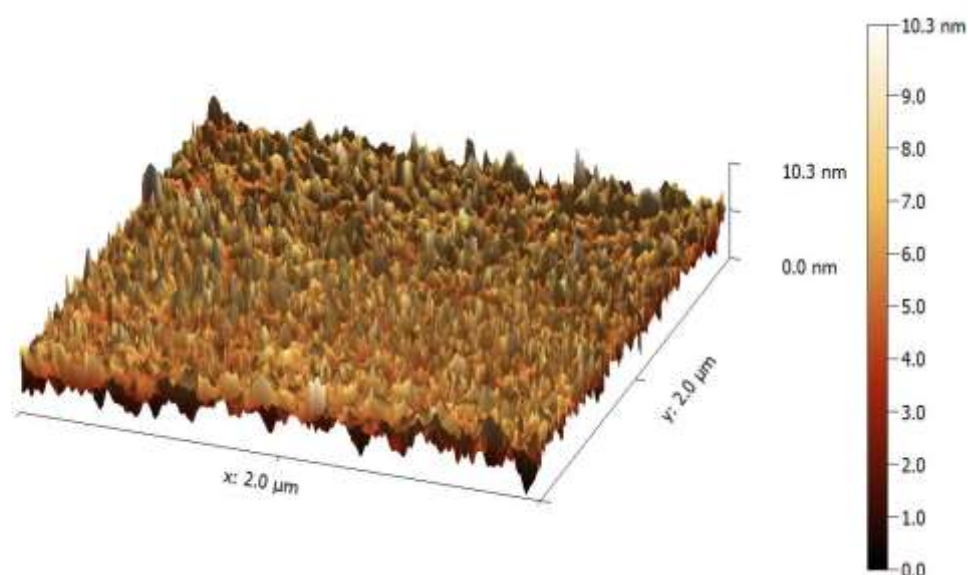


**Figure 1:** AFM 3D image of Cr<sub>2</sub>O<sub>3</sub> nanoparticles

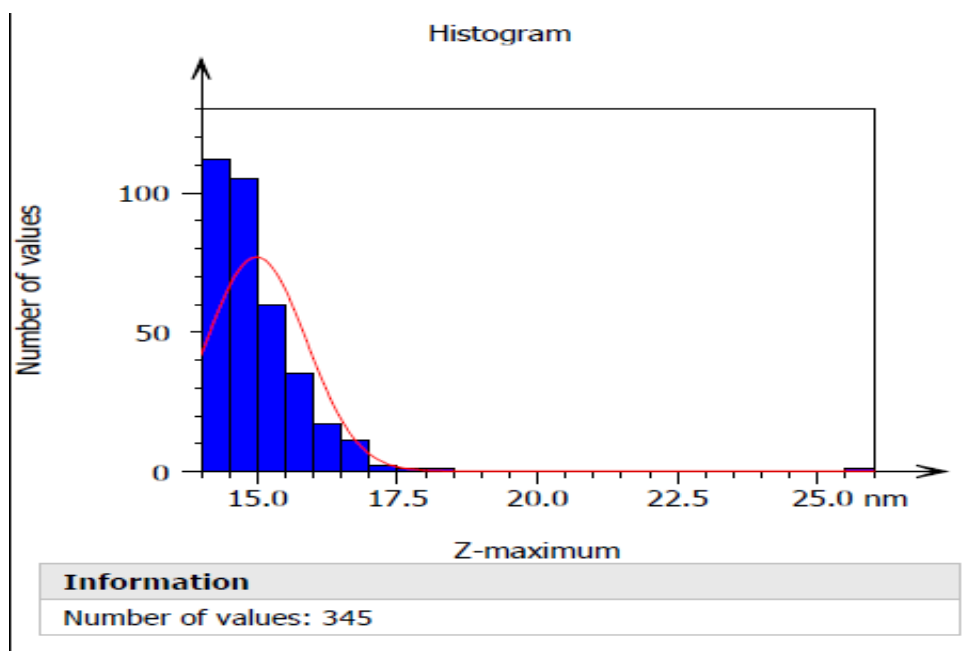


**Figure 2:** Cr<sub>2</sub>O<sub>3</sub> granularity cumulation distribution chart

### 3.2. Fe-SEM/EDX of PP composites nanostructured

As shown in Figure 3, SEM images of PP/Cr<sub>2</sub>O<sub>3</sub> nanocomposites revealed coatings with a globular shape and a nonhomogeneous spherical morphology [14].

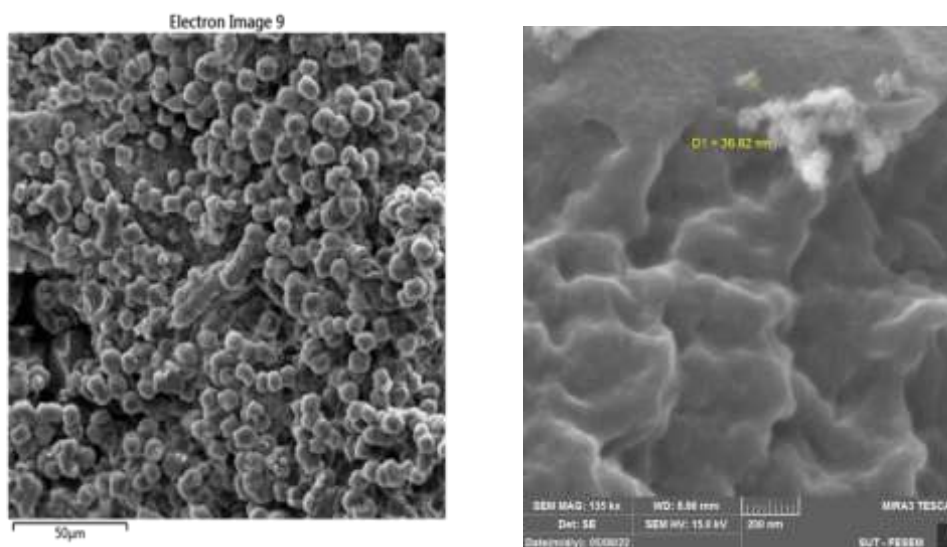


**Figure 3:** SEM images of PP/Cr<sub>2</sub>O<sub>3</sub> nanocomposite.

The EDX spectrum rise of PP/Cr<sub>2</sub>O<sub>3</sub> showed that the ratios of chrome, oxygen, and carbon are 4.2, 7.7, and 88.1%, respectively, as shown in Figure 4.

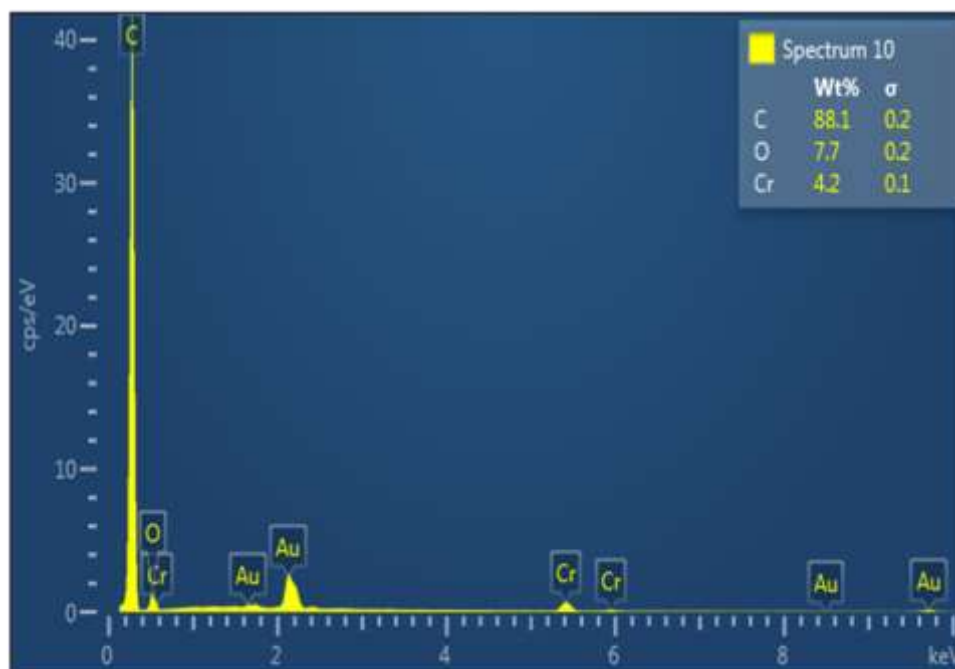


**Figure 4:** EDS of PP/Cr<sub>2</sub>O<sub>3</sub> nanocomposite

### 3.3. FT-IR of PP spectroscopy of PP composites nanostructured

The FT-IR spectrum of the PP/Cr<sub>2</sub>O<sub>3</sub> nanoparticle composite is reported in Figure 5. The bands at 3441 and 3385 cm<sup>-1</sup> belong to the stretching vibrations of the OH group of the interlayer, or absorbed water [15, 16]. The bands at 2961, 2924, and 2841 cm<sup>-1</sup> are attributed to the aliphatic C-H stretching. The bands at 1460 cm<sup>-1</sup> are indications of CH<sub>2</sub> deformation and are attributed to the bending vibration of the C-H bond. The strong band appeared at 1379 cm<sup>-1</sup> belongs to the symmetric CH<sub>3</sub> deformation. Furthermore, the absorptions at 1169, 1000, 976, and 843 cm<sup>-1</sup> are for isotactic polypropylene [17]. Finally, the band at 424 cm<sup>-1</sup> belongs to the Cr-O bond [18].

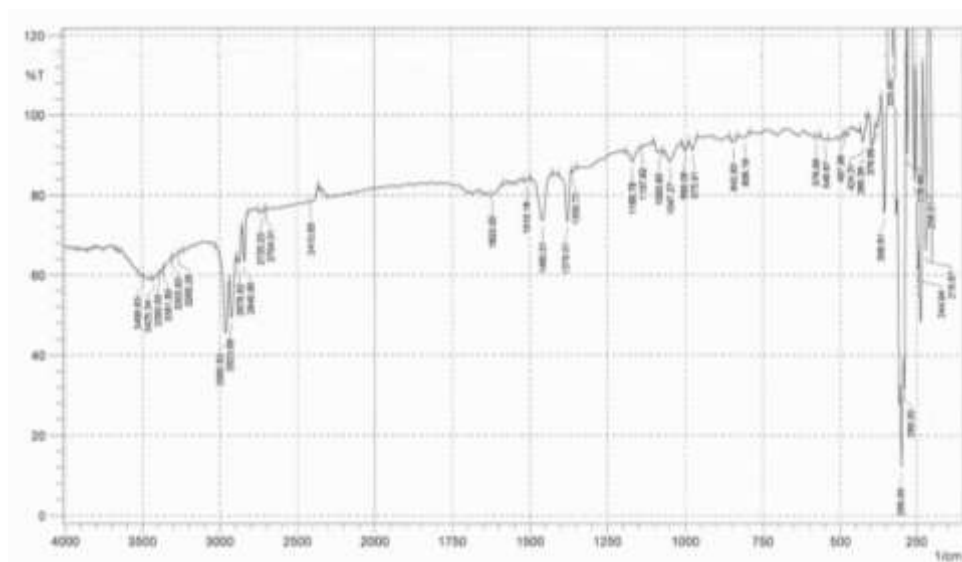


**Figure 5:** FT-IR spectrum of PP/Cr<sub>2</sub>O<sub>3</sub> nanoparticle composite

### 3.4. X-Ray diffraction of PP composites nanostructured

The portion of pure PP produces peaks at 14, 17, 18.5, 22, 26, and 28.5° on the XRD pattern of PP [19]. The XRD pattern of the PP/Cr<sub>2</sub>O<sub>3</sub> nanocomposite is shown in Figure 6. The peaks

refer to trigonal (hexagonal axes) chromium oxide with ICDD card no.96.901.5654. The  $\text{Cr}_2\text{O}_3$  standard reference was observed at  $2\theta = 42.6358^\circ$  and indexed at 311 as shown in Tables 2A and 2B [20].

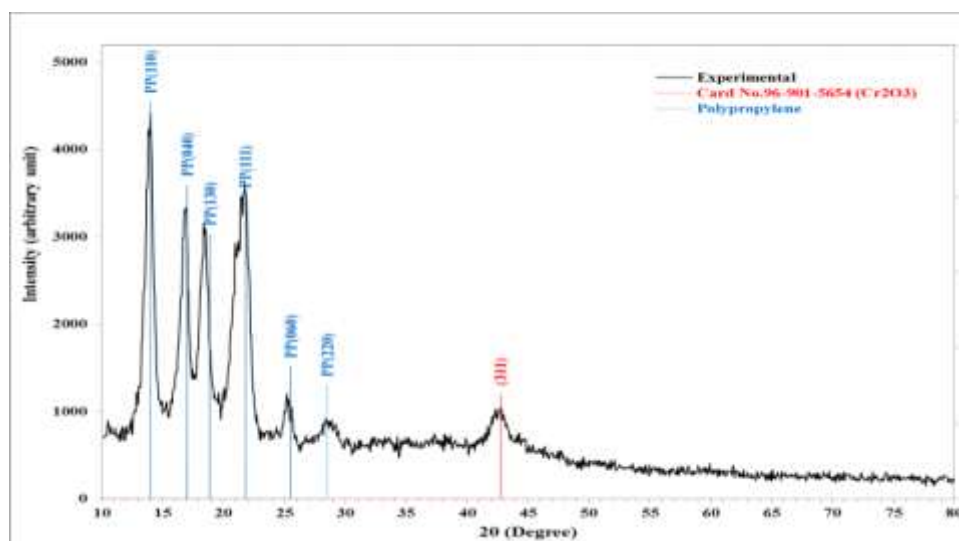


**Figure 6:** X-Ray diffraction pattern of PP/ $\text{Cr}_2\text{O}_3$

**Table 2A :** The structure parameters of PP/ $\text{Cr}_2\text{O}_3$  as obtained from XRD analysis

$2\theta$ (Degree)	FWHM (Degree)	$d_{hkl}$ Experimental ( $\text{\AA}$ )	G.S (nm)	Phase	hkl
13.8675	0.7417	6.1845	11.5	PP	(110)
16.8344	0.6887	5.1563	13.5	PP	(040)
18.3709	0.6887	4.7242	12.5	PP	(130)
21.8675	1.3245	4.0301	10.2	PP	(111)
25.2053	0.6887	3.4696	13.7	PP	(060)
28.543	1.3245	3.1000	9.2	PP	(220)
42.6358	1.4304	2.67423	14.0	Hexagonal $\text{Cr}_2\text{O}_3$	(311)

**Table 2B :** Crystallographic data of  $\text{Cr}_2\text{O}_3$

Name	chromium oxide
Mineral Name	Eskolaite
Formula	$\text{Cr}_2\text{O}_3$
I/Cor	2.59
Sample .N	9015653
Quality	C-calculated

Crystallographic data							
Space group	R -3 c (167)						
Crystal system	trigonal (hexagonal axes)						
Cell parameters	a = 4.8152 $\text{\AA}$ , c = 13.2420 $\text{\AA}$						
Atom coordinates	Element	Oxide	x	y	z	Bi	Focc
	Cr		0	0	0.347	0.544	1
	O		0.311	0	0.25	0.631	1

Physical Properties	
Calculated density	5.69500 $\text{g/cm}^3$

### 3.5. Thermogravimetric analyses (TG and DSC) of PP composites nanostructured

Thermogravimetric analysis (TG) is a technique that can provide information about the amount of organic material present in composite interlayers [21]. TGA can also show how too much surface modification results in a lower thermal degradation temperature and an assortment of negative effects on the composite properties [22]. The nanocomposite PP/Cr<sub>2</sub>O<sub>3</sub> synthesized by the green method was decomposition in three stages as follows:

- 1- First stage at 50-250 °C with including water loss, which adsorbed physically of the nanocomposite and proved to lose a small amount of its components at the same temperature compared to the previous nanocomposite.
- 2- Second stage occurs at 250-450 °C with a total weight of 73.35%, this stage includes the start of the loss of propylene units and the decomposition of the carbon skeleton of the polymer [23].
3. The third stage begins at a temperature greater than 800 °C and has a weight of 26.65%; this stage is caused by the amount of Cr<sub>2</sub>O<sub>3</sub> NPs. Figure 7 shows the three stages of the decomposition.

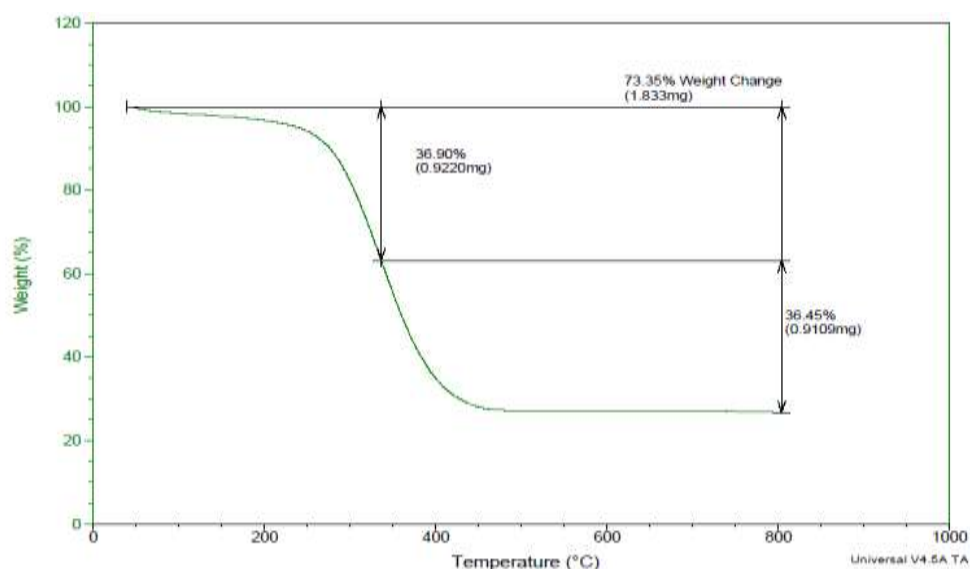


**Figure 7:** TG curve of PP/Cr<sub>2</sub>O<sub>3</sub>

Differential scanning calorimetry analysis of the polypropylene nano-metal oxide PP/Cr<sub>2</sub>O<sub>3</sub> was synthesized by the green method. The nanocomposites have two endothermic stages. First, at 243.95 °C, it is considered the glass transition of polypropylene in nanocomposites in comparison with the standard reference of polypropylene, which is -20 °C [24]. Second, 415.41 °C is conceded to the melting point of polypropylene in nanocomposites in comparison with the standard reference for polypropylene, which is 160 °C [25]. This is another indication of the success of the reaction, as shown in Figure (8).

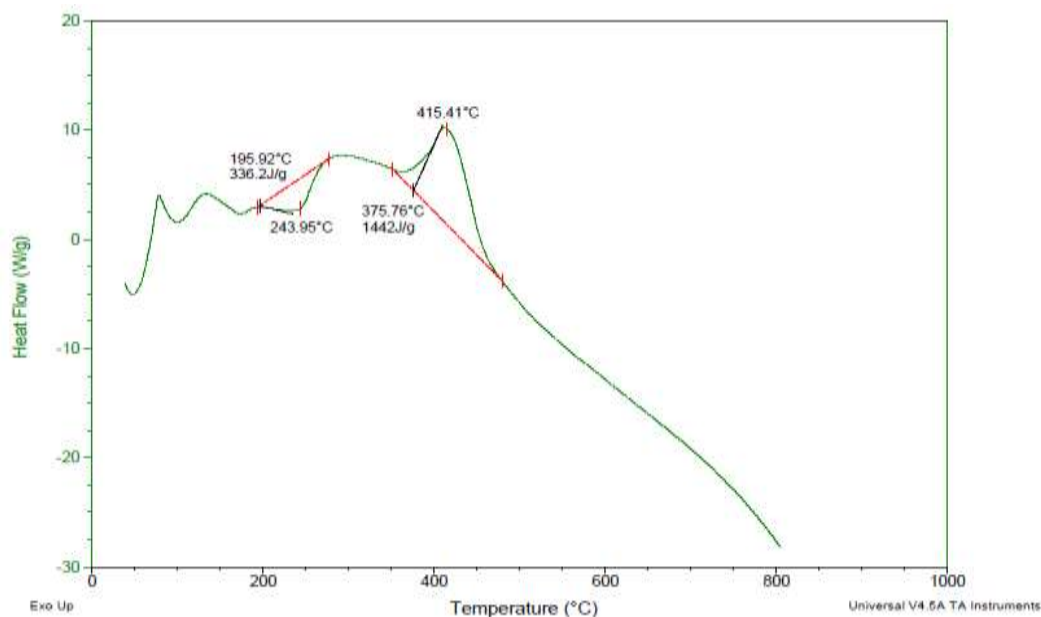


**Figure 8:** DSC curve of PP/Cr<sub>2</sub>O<sub>3</sub>

#### 4. Antibacterial and antifungal activities

Antibacterial tests were performed, and the straight inhibitory effect of nanocomposites was established on cultures of reference strains of about 100  $\mu$ L of selected gram-positive bacteria [*Bacillus subtilis* (+)]. The activity of the nanocomposites was calculated in three dilutions by the method of spreading the disc into Petri dishes with a diameter of 20 mL. The Petri dishes were placed inverted and kept in an incubator at a constant temperature of 37 °C for 18-24 hours (depending on the type of microorganism tested). The diameter of the bacterial growth inhibition zones was measured by nanocomposites from the edge of the film to the end of the absence zone. This was measured through photographs of dishes (Figure 9) [26], and exhibited an activity as shown in Table 3. It has been observed that nanocomposites have high levels of antibacterial activity.

**Table 3 :** Inhibitory effect on PP nanocomposite

Sample number	Nanocomposite formula	Bacterial inhibition by dilution of nanocomposites		
		25%	50%	75%
8	PP/Cr <sub>2</sub> O <sub>3</sub>	10 mm	12 mm	11 mm

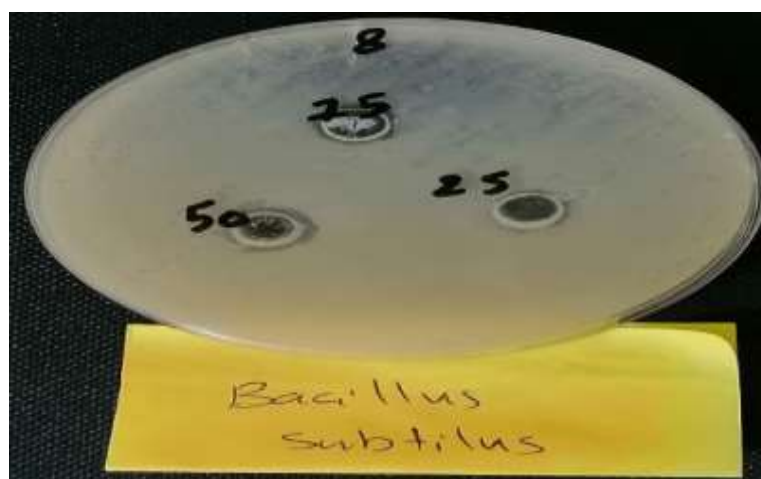


**Figure 9:** Inhibition of bacteria on PP nanocomposite

An *In vitro* assay was performed on the type of growth medium (PDA). The straight inhibitory effect of nanocomposites was measured in about 100  $\mu$ l of *Candida albicans* by the disk diffusion method in 20 mL on Petri dishes, which were placed inverted and kept in an incubator at a constant temperature of 28 °C for 72 hours. The fungi-containing Petri dish's diameter was measured. The growth inhibition region of the fungi was calculated from the edge of the film to the end of the absence region of the measurement [27]. The results showed that the growth fungus inhibition areas of the nanocomposite were 38 mm.

## 5. Antioxidant activity

### 5.1. 1,1-Diphenyl-2-picryl hydrazyl (DPPH)

In a test tube, a solution of 1,1-diphenyl-2-picryl hydrazyl (DPPH) (4 mg) in methanol (100 mL) was coated with aluminum foil. The solution was kept shielded from light. Various concentrations (100, 50, 25, 12.5, and 6.25 ppm) were prepared by dissolving the tested compound (1 mg) in methanol (10 mL) to prepare 100 ppm. This concentration was then diluted to prepare the above-mentioned concentrations.

#### 5.1.2. Ascorbic acid

Similar concentrations to those prepared in the previous procedure were prepared. The radical-scavenging effect of the stable free-radical DPPH was assessed, and the process was appraised for the antioxidant efficacy of the plant methanol extract and normal vitamin C. In a test tube, 1 mL of the diluted or normal solution (100, 50, 25, 12.5, and 6.25 ppm) was applied to the DPPH solution (1 mL). Using a spectrophotometer, the absorption of all solvents was measured at 517 nm, and then they were incubated at 37 °C for just 1 hour. Three measurements were made using Equation 1. It is able to determine the potential to scavenge DPPH [28].

$$I\% = [\text{Abs blank} - \text{Abs sample}] / \text{Abs blank} \times 100 \quad (1)$$

The newly synthesized nanocomposite showed antioxidant activity against the DPPH free radical and gave a good scavenging percentage. As a result, the tested nanocomposite showed antioxidant properties and was selected for further testing. Accordingly, inhibitory concentration ( $IC_{50}$ ) values were recorded and listed in Table 4. It is clear from this work that the nanocomposite has average antioxidant activity, with variation in the results shown in Table 4 and Figure 10.

**Table 4 :** DPPH radical scavenging activity for PP/Cr<sub>2</sub>O<sub>3</sub> nanocomposite with ascorbic acid

PP nano composite	Concentration $\mu$ g/mL					R <sup>2</sup>	Linear equation	Ic50
	6.250	12.50	25.00	50.00	100.00			
PP/Cr <sub>2</sub> O <sub>3</sub>	6.84	25.78	31.05	34.21	46.31	0.7425	y = 0.326x + 16.205	103.6
Ascorbic acid	51.4	57.4	61.1	64.7	93.2	0.9572	y = 0.416x + 49.433	1.4

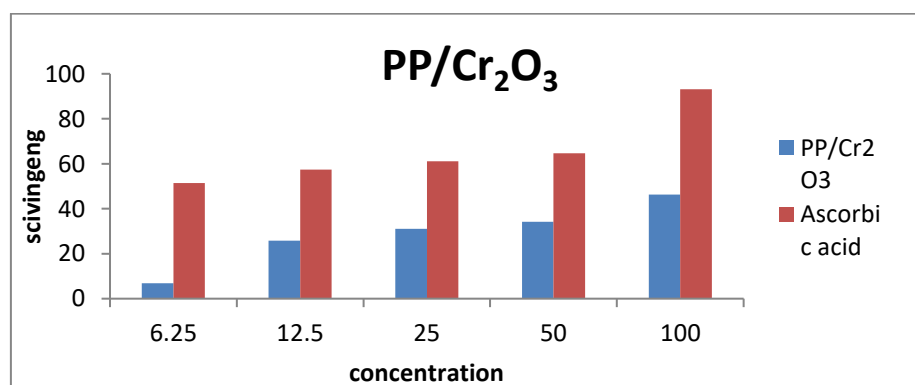


**Figure 10:** Antioxidant activity of PP/Cr<sub>2</sub>O<sub>3</sub> using the DPPH assay

## 6. Conclusion

In this work, the biosynthesis of Cr<sub>2</sub>O<sub>3</sub> NPs from licorice root extract (*Glycyrrhiza glabra*) was mixed with a polypropylene polymer to obtain nanocomposites (PP/NPs). AFM, SEM, EDX, FTIR, XRD, TG, and DSC measurements were performed, and the results of the measurements showed that the compounds were manufactured in the form of nanoparticles.

The AFM technology revealed that these nanocomposites' particles are fewer than 100 nanometers in size and dimension. The images also reveal that the grooves in the nanostructures are not homogeneous, owing to the formation of a coating layer over and between the polypropylene. The anti-bacterial and anti-fungal activities of the mentioned composites were investigated, as well as the area of microorganism growth retardation and antioxidant results.

## References

- [1] R. Chokkareddy, G. G. Redhi, S. Kanchi, and S. Ahmed, "Green synthesis of metal nanoparticles and its reaction mechanisms", *Green Metal Nanoparticles*, pp. 113-139, 2018.
- [2] A. Alwash, "The green synthesise of zinc oxide catalyst using pomegranate peels extract for the photocatalytic degradation of methylene blue dye," *Baghdad Sci J. 2021Sep*, vol. 12, no. 17, p. 3, 2020.
- [3] I. M. Chung, I. Park, K. S. Hyun, M. Thiruvengadam, and G. Rajakumar, "Plant-mediated synthesis of silver nanoparticles: their characteristic properties and therapeutic applications", *Nanoscale Research Letters*, vol. 11, no. 1, pp. 1-14, 2016.
- [4] M. A. Al-Shaheen, M. N. Owaid, and R. F. Muslim, "Synthesis and characterization of zinc nanoparticles by natural organic compounds extracted from licorice root and their influence on germination of sorghum bicolor seeds", *Jordan Journal of Biological Sciences*, vol. 13, no. 4, pp. 559-565, 2020.
- [5] D. Ahmed and B. I. Al-Abdaly, "Effect of SiO<sub>2</sub> Addition and Calcination Temperature on Surface Area, Crystal Size, Particles Size and Phase Transformation of TiO<sub>2</sub> Prepared by Sol-Gel Method," *Solid State Technology*, vol. 64, no. 2, pp. 3945-3959, 2021.
- [6] D. Cho, H. Zhou, Y. Cho, D. Audus, and Y. L. Joo, "Structural properties and superhydrophobicity of electrospun polypropylene fibers from solution and melt", *Polymer*, vol. 51, no. 25, pp. 6005-6012, 2010.
- [7] T. Czigány and F. Ronkay, "Editorial corner - a personal view", *eXPRESS Polymer Letters*, vol. 14, no. 6, p. 510-511, 2020.
- [8] S. Yin, R. Tuladhar, R. A. Shanks, T. Collister, M. Combe, M. Jacob, M. Tian, and N. Sivakugan, "Fiber preparation and mechanical properties of recycled polypropylene for reinforcing concrete", *Journal of Applied Polymer Science*, vol. 132, no. 16, Article number 41866 (10 pages), 2015.
- [9] F. Nogueira, P. Teixeira, and I. C. Gouveia, "Electrospinning polypropylene with an amino acid as a strategy to bind the antimicrobial peptide Cys-LC-LL-37", *Journal of Materials Science*, vol. 53, no. 6, pp. 4655-4664, 2018.
- [10] A. Corciova, A. F. Burlec, A. M. Gheldiu, A. Fifere, A. L. Lungoci, N. Marangoci, and C. Mircea, "Biosynthesis of silver nanoparticles using licorice extract and evaluation of their antioxidant activity", *Revista de Chimie*, vol. 70, no. 11, pp. 4053-4056, 2019.
- [11] M. Ramazanov and F. Hajiyeva, "Copper and copper oxide nanoparticles in polypropylene matrix: Synthesis, characterization, and dielectric properties", *Composite Interfaces*, vol. 27, no. 11, pp. 1047-1060, 2020.
- [12] S. A. Habeeb and K. A. Saleh, "Electrochemical polymerization and biological activity of 4-(nicotinamido)-4-oxo-2-butenic acid as an anticorrosion coating on A 316L stainless steel surface", *Iraqi Journal of Science*, vol. 62, no. 3, pp. 729-741, 2021.
- [13] A. S. Elewi, S. A. W. Al-Shammaree, and A. K. M. A. Sammarraie, "Hydrogen peroxide biosensor based on hemoglobin-modified gold nanoparticles–screen printed carbon electrode," *Sensing and Bio-Sensing Research*, vol. 28, p. 100340, 2020.
- [14] K. A. Saleh and M. I. Ali, "Electro polymerization for (N-terminal tetrahydrophthalamic acid) for anti-corrosion and biological activity applications", *Iraqi Journal of Science*, vol. 61, no. 1, pp. 1-12, 2020.

- [15] A. R. Salih and Z. A. Al-Messri, "Synthesis, characterization and evaluation of some pyranopyrazole derivatives as multifunction additives for medium lubricating oils", *Iraqi Journal of Science*, vol. 63, no. 7, pp. 2827-2838, 2022.
- [16] A. H. Al-Husseini, W. R. Saleh, and A. M. Al-Sammarraie, "A specific NH<sub>3</sub> gas sensor of a thick MWCNTs-OH network for detection at room temperature," *Journal of Nano Research*, vol. 56, pp. 98-108, 2019.
- [17] M. R. Jung, F. D. Horgen, S. V. Orski, V. Rodriguez, K. L. Beers, G. H. Balazs, T. T. Jones, T. M. Work, K. C. Brignac, S. J. Royer, K. D. Hyrenbach, B. A. Jensen, and J. M. Lynch, "Validation of ATR FT-IR to identify polymers of plastic marine debris, including those ingested by marine organisms", *Marine Pollution Bulletin*, vol. 127, vol. 63, no. 7, pp. 704-716, 2018.
- [18] J. Singh, V. Verma, R. Kumar, S. Sharma, and R. Kumar, "Effect of structural and thermal disorder on the optical band gap energy of Cr<sub>2</sub>O<sub>3</sub> nanoparticles," *Materials Research Express*, vol. 6, no. 8, p. 085039, 2019.
- [19] S. H. Yetgin, "Effect of multi walled carbon nanotube on mechanical, thermal and rheological properties of polypropylene", *Journal of Materials Research and Technology*, vol. 8, no. 5, pp. 4725-4735, 2019.
- [20] M. S. Zoromba, S. Alghool, S. Abdel-Hamid, M. Bassyouni, and M. Abdel-Aziz, "Polymerization of aniline derivatives by K<sub>2</sub>Cr<sub>2</sub>O<sub>7</sub> and production of Cr<sub>2</sub>O<sub>3</sub> nanoparticles", *Polymers for Advanced Technologies*, vol. 28, no. 7, pp. 842-848, 2017.
- [21] Z. A. A. Latif, A. M. Mohammed, and N. M. Abbass, "Synthesis and characterization of polymer nanocomposites from methyl acrylate and metal chloride and their application," *Polymer Bulletin*, vol. 77, pp. 5879-5898, 2020.
- [22] M. Al-Samhan, J. Samuel, F. Al-Attar, and G. Abraham, "Comparative effects of MMT clay modified with two different cationic surfactants on the thermal and rheological properties of polypropylene nanocomposites", *International Journal of Polymer Science*, vol. 2017, Article number. 5717968, (9 pages), 2017.
- [23] D. Li, L. Zhou, X. Wang, L. He, and X. Yang, "Effect of crystallinity of polyethylene with different densities on breakdown strength and conductance property", *Materials*, vol. 12, no. 11, p. 1746, 2019.
- [24] C. L. de Carvalho, A. F. Silveira, and D. d. S. Rosa, "A study of the controlled degradation of polypropylene containing pro-oxidant agents", *SpringerPlus*, vol. 2, no. 1, pp. 1-11, 2013.
- [25] P. V. Joseph, K. Joseph, S. Thomas, C. K. S. Pillai, V. S. Prasad, G. Groeninckx, and M. Sarkissova, "The thermal and crystallisation studies of short sisal fibre reinforced polypropylene composites," *Composites Part A: Applied Science and Manufacturing*, vol. 34, no. 3, pp. 253-266, 2003.
- [26] T. G. Volova, A. A. Shumilova, I. P. Shidlovskiy, E. D. Nikolaeva, A. G. Sukovaty, A. D. Vasiliev, and E. I. Shishatskaya, "Antibacterial properties of films of cellulose composites with silver nanoparticles and antibiotics", *Polymer Testing*, vol. 65, pp. 54-68, 2018.
- [27] S. W. Kim, J. H. Jung, K. Lamsal, Y. S. Kim, J. S. Min, and Y. S. Lee, "Antifungal effects of silver nanoparticles (AgNPs) against various plant pathogenic fungi", *Mycobiology*, vol. 40, no. 1, pp. 53-58, 2012.
- [28] R. Amarowicz, R. Pegg, P. R. Moghaddam, B. Barl, and J. Weil, "Free-radical scavenging capacity and antioxidant activity of selected plant species from the canadian prairies", *Food chemistry*, vol. 84, no. 4, pp. 551-562, 2004.